INTERNATIONAL JOURNAL FOR NUMERICAL METHODS IN ENGINEERING
Int. J. Numer. Meth. Engng (2010)
Published online in Wiley Online Library (wileyonlinelibrary.com). DOI: 10.1002/nme.3007

Dynamics of clusters of charged particulates in electromagnetic fields

T. I. Zohdi*, †

Department of Mechanical Engineering, 6195 Etcheverry Hall, University of California, Berkeley, CA 94720-1740, U.S.A.

SUMMARY

The dynamics of rigid clusters of charged particulates is the subject of this work. The work ascertains what properties of the cluster control its dynamic response to an external electromagnetic field. A primary focus is on the role of the distribution of the charges within the cluster and the effects of the Lorentz force on the overall body's linear and angular momentum. The presentation contains a derivation of the equations governing a charged cluster's dynamics and development of corresponding numerical methods for the simulation. Numerical examples are presented, along with comparisons to qualitative analytical results, where possible. Copyright © 2010 John Wiley & Sons, Ltd.

Received 24 March 2010; Revised 2 June 2010; Accepted 30 June 2010

KEY WORDS: particulates; clusters; charged; dynamics

1. INTRODUCTION

Flowing, small-scale particulates are ubiquitous in industrial processes and in the natural sciences.‡ Applications include electrostatic copiers, inkjet printers, powder coating machines, etc. and a variety of small-scale manufacturing processes (see, for example, Luo and Dornfeld [1–4], Arbelaez *et al.* [5, 6], Ciampini *et al.* [7, 8], Gomes-Ferreira *et al.* [9] and Ghobeity *et al.* [10, 11]). At small scales, particulates exhibit strong sensitivity to inter-particle near-field forces, which are a result of inter-particle electromagnetic forces, leading to agglomeration and cluster formation. Clustering is an inevitable and frequently unwanted occurrence in such systems (Figure 1). These clusters can lead to manufacturing inconsistencies/variability that can strongly affect the overall product

*Correspondence to: T. I. Zohdi, Department of Mechanical Engineering, 6195 Etcheverry Hall, University of California, Berkeley, CA 94720-1740, U.S.A.
†E-mail: zohdi@me.berkeley.edu
‡The term 'particulates', which usually refers to small-scale particles, will be used interchangeably with the term 'particle'.

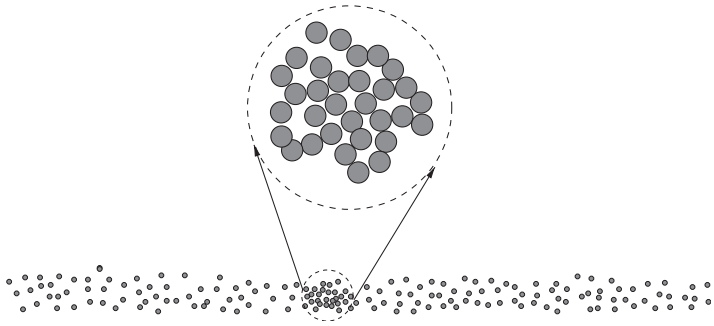

Figure 1. Agglomeration of material (formation of a cluster) within a flow of particulates.

quality, in particular if the manufactured devices have small dimensions.[§] External electromagnetic fields can be utilized to manipulate and control small scale, charged particulates that are used in industrial processes, in order to achieve results that are not possible by purely mechanical means alone. This paper is concerned with identifying what controls the dynamics of clusters that are present in such systems, in particular when they interact with external electromagnetic fields.

In this work, we consider the cluster to be already formed, with particles rigidly bound together by either mechanical, chemical or electromagnetic bonds. Investigation of the evolution of such clusters from loose, free-flowing particulates can be found in Zohdi [15–24], and is outside the scope of the present work, although a brief discussion of cluster formation will be given toward the end of the presentation. Such clusters possess unique dynamics that are important in order to understand and fully control relevant industrial processes, as well as from a purely fundamental point of view. Of particular interest is to compare and contrast the differences in the dynamics of a cluster of charged particles and that of a (hypothetical) single charged particle (with the same overall charge) whose motion is governed by

$$m\dot{\boldsymbol{v}} = q(\boldsymbol{E}^{\text{ext}} + \boldsymbol{v} \times \boldsymbol{B}^{\text{ext}}), \tag{1}$$

where m is the mass of the particle, $\boldsymbol{v}$ is the particle velocity, $\boldsymbol{E}^{\text{ext}} = (E_1^{\text{ext}}, E_2^{\text{ext}}, E_3^{\text{ext}})$ is the external electric field and $\boldsymbol{B}^{\text{ext}} = (B_1^{\text{ext}}, B_2^{\text{ext}}, B_3^{\text{ext}})$ is the external magnetic field.

2. DYNAMICS OF CHARGED CLUSTERS

Consider a collection of rigidly bonded particles, $i = 1, 2, \ldots, N_c$, in a cluster (Figure 2). The individual particle dynamics are described by (which leads to a coupled system)

$$m_i \ddot{\boldsymbol{r}}_i = \underbrace{\boldsymbol{\psi}_i^{\text{tot}}}_{\text{total forces}} = \underbrace{\boldsymbol{\psi}_i^{\text{int}}}_{\text{internal forces}} + \underbrace{\boldsymbol{\psi}_i^{\text{ext}}}_{\text{external forces}} = \boldsymbol{\psi}_i^{\text{int}} + \underbrace{q_i(\boldsymbol{E}^{\text{ext}} + \boldsymbol{v}_i \times \boldsymbol{B}^{\text{ext}})}_{\boldsymbol{\psi}_i^{\text{ext}}}, \tag{2}$$

[§]For a review of the effects of clusters on the macroscale material properties of solids that contain them, see Torquato [12], as well as Ghosh *et al.* [13] for domain partitioning methods that are capable of handling materials with general non-uniform microstruture. For a review of the state of the art on multiscale methods that bridge scales, with applications to nanotechnology, see Fish [14].

DOI: 10.1002/nme

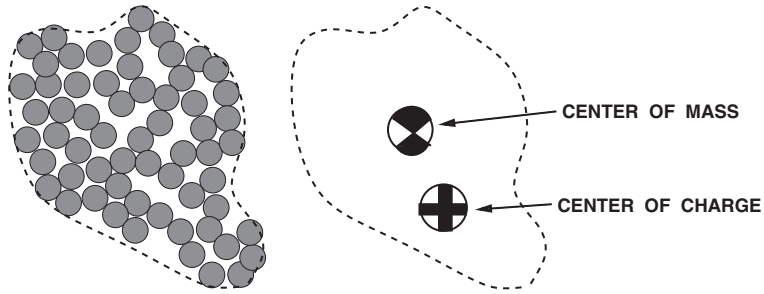

Figure 2. A collection of charged particles that are rigidly bonded together. The nature of the particle-to-particle bonding (mechanical, electronic, chemical, etc.) is irrelevant in the present analysis. The mass-center and 'charge' center will generally not coincide. This difference will lead to a variation in the dynamics of the center-of-mass of a cluster relative to a single charged particle of equal mass and charge, strongly influenced by the equation of overall balance of angular momentum.

where $\boldsymbol{r}_i$ is the position vector of the ith particle, m_i is the mass of a single particle and $\boldsymbol{\psi}_i^{\text{tot}}$ is the sum of the forces acting on the ith particle, due to other particles in the system ('internal' particle-to-particle near-fields, bonding forces, etc., $\boldsymbol{\psi}_i^{\text{int}}$) and due to the external electric and magnetic fields ($\boldsymbol{\psi}_i^{\text{ext}}$).

Remarks

Although the exact nature of particle-to-particle interaction is not important in the present (overall motion) analysis, since the corresponding forces are internal to the system, in passing, we mention that there are a variety of possible interparticle representations for loose, free-flowing, charged particles. We refer the reader to Frenklach and Carmer [25], Haile [26], Hase [27], Schlick [28], Rapaport [29], Torquato [30], Rechtsman *et al.* [31, 32] and Zohdi [15–24] for overviews of the various representations for particle interaction, such as those based on the familiar Mie, Lennard-Jones, and Morse potentials (see Moelwyn-Hughes [33] for reviews). Also, three-body terms can be introduced directly into the inter-particle interaction [34] or via term-wise modifications to the two-body representations [35].

2.1. Group dynamics of a rigidly bound collection of particles

When we consider a collection of particles that are bound together as a rigid body, the exact nature of the internal particle-to-particle interaction is irrelevant to the overall system dynamics, since the internal forces in the system are equal in magnitude and opposite in direction, leading to

$$\sum_{i=1}^{N_c}(\boldsymbol{\psi}_i^{\text{ext}}+\boldsymbol{\psi}_i^{\text{int}})=\sum_{i=1}^{N_c}\boldsymbol{\psi}_i^{\text{ext}}+\underbrace{\sum_{i=1}^{N_c}\boldsymbol{\psi}_i^{\text{int}}}_{=\mathbf{0}}=\sum_{i=1}^{N_c}\boldsymbol{\psi}_i^{\text{ext}}\stackrel{\text{def}}{=}\boldsymbol{\Psi}^{\text{EXT}}, \tag{3}$$

where $\boldsymbol{\Psi}^{\text{EXT}}$ is the overall external force acting on the cluster. The position vector of the center of mass of the system is given by

$$\boldsymbol{r}_{\text{cm}}\stackrel{\text{def}}{=}\frac{\sum_{i=1}^{N_c}m_i\boldsymbol{r}_i}{\sum_{i=1}^{N_c}m_i}=\frac{1}{\mathscr{M}}\sum_{i=1}^{N_c}m_i\boldsymbol{r}_i, \tag{4}$$

DOI: 10.1002/nme

where $\mathscr{M}$ is the total system mass. A decomposition of the position vector for particle i, of the form $\boldsymbol{r}_i = \boldsymbol{r}_{\rm cm} + \boldsymbol{r}_{{\rm cm}\rightarrow i}$, allows the linear momentum of the system of particles ($\boldsymbol{G}$) to be written as

$$\sum_{i=1}^{N_{\rm c}} \underbrace{m_i \dot{\boldsymbol{r}}_i}_{\boldsymbol{G}_i} = \sum_{i=1}^{N_{\rm c}} m_i (\dot{\boldsymbol{r}}_{\rm cm} + \dot{\boldsymbol{r}}_{{\rm cm}\rightarrow i}) = \sum_{i=1}^{N_{\rm c}} m_i \dot{\boldsymbol{r}}_{\rm cm} = \dot{\boldsymbol{r}}_{\rm cm} \sum_{i=1}^{N_{\rm c}} m_i = \mathscr{M} \dot{\boldsymbol{r}}_{\rm cm} \stackrel{\rm def}{=} \boldsymbol{G}_{\rm cm}, \tag{5}$$

since $\sum_{i=1}^{N_{\rm c}} m_i \dot{\boldsymbol{r}}_{{\rm cm}\rightarrow i} = \boldsymbol{0}$. Furthermore, $\dot{\boldsymbol{G}}_{\rm cm} = \mathscr{M} \ddot{\boldsymbol{r}}_{\rm cm}$; thus

$$\dot{\boldsymbol{G}}_{\rm cm} = \mathscr{M} \ddot{\boldsymbol{r}}_{\rm cm} = \sum_{i=1}^{N_{\rm c}} \boldsymbol{\psi}_i^{\rm ext} = \sum_{i=1}^{N_{\rm c}} q_i (\boldsymbol{E}^{\rm ext} + \boldsymbol{v}_i \times \boldsymbol{B}^{\rm ext}) \stackrel{\rm def}{=} \boldsymbol{\Psi}^{\rm EXT}. \tag{6}$$

The angular momentum relative to the center-of-mass can be written as (utilizing $\dot{\boldsymbol{r}}_i = \boldsymbol{v}_i = \boldsymbol{v}_{\rm cm} + \boldsymbol{v}_{{\rm cm}\rightarrow i}$)

$$\boldsymbol{H}_{\rm cm} = \sum_{i=1}^{N_{\rm c}} (\boldsymbol{r}_{{\rm cm}\rightarrow i} \times m_i \boldsymbol{v}_{{\rm cm}\rightarrow i}) = \sum_{i=1}^{N_{\rm c}} (\boldsymbol{r}_{{\rm cm}\rightarrow i} \times m_i (\boldsymbol{v}_i - \boldsymbol{v}_{\rm cm})) \tag{7}$$

$$= \sum_{i=1}^{N_{\rm c}} (m_i \boldsymbol{r}_{{\rm cm}\rightarrow i} \times \boldsymbol{v}_i) - \left(\underbrace{\sum_{i=1}^{N_{\rm c}} m_i \boldsymbol{r}_{{\rm cm}\rightarrow i}}_{=0} \right) \times \boldsymbol{v}_{\rm cm}, \tag{8}$$

and since $\boldsymbol{v}_{{\rm cm}\rightarrow i} = \boldsymbol{\omega} \times \boldsymbol{r}_{{\rm cm}\rightarrow i}$ for a rigid body,

$$\boldsymbol{H}_{\rm cm} = \sum_{i=1}^{N_{\rm c}} m_i (\boldsymbol{r}_{{\rm cm}\rightarrow i} \times \boldsymbol{v}_{{\rm cm}\rightarrow i}) = \sum_{i=1}^{N_{\rm c}} \underbrace{m_i (\boldsymbol{r}_{{\rm cm}\rightarrow i} \times (\boldsymbol{\omega} \times \boldsymbol{r}_{{\rm cm}\rightarrow i}))}_{\stackrel{\rm def}{=} \boldsymbol{H}_{{\rm cm}\rightarrow i}}. \tag{9}$$

Decomposing the relative position vector into its components

$$\boldsymbol{r}_{{\rm cm}\rightarrow i} = \boldsymbol{r}_i - \boldsymbol{r}_{\rm cm} = \hat{x}_{i1} \boldsymbol{e}_1 + \hat{x}_{i2} \boldsymbol{e}_2 + \hat{x}_{i3} \boldsymbol{e}_3, \tag{10}$$

where $\hat{x}_{i1}$, $\hat{x}_{i2}$ and $\hat{x}_{i3}$ are the coordinates of the mass points measured *relative to the center-of-mass*, and expanding the angular momentum expression, yields

$$H_1 = \omega_1 \sum_{i=1}^{N_{\rm c}} (\hat{x}_{i2}^2 + \hat{x}_{i3}^2) m_i - \omega_2 \sum_{i=1}^{N_{\rm c}} \hat{x}_{i1} \hat{x}_{i2} m_i - \omega_3 \sum_{i=1}^{N_{\rm c}} \hat{x}_{i1} \hat{x}_{i3} m_i \tag{11}$$

and

$$H_2 = -\omega_1 \sum_{i=1}^{N_{\rm c}} \hat{x}_{i1} \hat{x}_{i2} m_i + \omega_2 \sum_{i=1}^{N_{\rm c}} (\hat{x}_{i1}^2 + \hat{x}_{i3}^2) m_i - \omega_3 \sum_{i=1}^{N_{\rm c}} \hat{x}_{i2} \hat{x}_{i3} m_i \tag{12}$$

and

$$H_3 = -\omega_1 \sum_{i=1}^{N_{\rm c}} \hat{x}_{i1} \hat{x}_{i3} m_i - \omega_2 \sum_{i=1}^{N_{\rm c}} \hat{x}_{i2} \hat{x}_{i3} m_i + \omega_3 \sum_{i=1}^{N_{\rm c}} (\hat{x}_{i1}^2 + \hat{x}_{i2}^2) m_i, \tag{13}$$

DOI: 10.1002/nme

which can be concisely written as

$$\boldsymbol{H}_{\mathrm{cm}}=\overline{\boldsymbol{I}}\cdot\boldsymbol{\omega}, \tag{14}$$

where we define the moments of inertia with respect to the center-of-mass

$$\overline{I}_{11}=\sum_{i=1}^{N_c}(\hat{x}_{i2}^2+\hat{x}_{i3}^2)m_i,\quad \overline{I}_{22}=\sum_{i=1}^{N_c}(\hat{x}_{i1}^2+\hat{x}_{i3}^2)m_i,\quad \overline{I}_{33}=\sum_{i=1}^{N_c}(\hat{x}_{i1}^2+\hat{x}_{i2}^2)m_i, \tag{15}$$

$$\overline{I}_{12}=\overline{I}_{21}=-\sum_{i=1}^{N_c}\hat{x}_{i1}\hat{x}_{i2}m_i,\quad \overline{I}_{23}=\overline{I}_{32}=-\sum_{i=1}^{N_c}\hat{x}_{i2}\hat{x}_{i3}m_i,\quad \overline{I}_{13}=\overline{I}_{31}=-\sum_{i=1}^{N_c}\hat{x}_{i1}\hat{x}_{i3}m_i. \tag{16}$$

The particles' own inertia contribution about their respective mass-centers to the overall moment of inertia of the agglomerated body can be described by the Huygens–Steiner (generalized 'parallel axis' theorem) formula ($p,s=1,2,3$)

$$\bar{I}_{ps}=\sum_{i=1}^{N_c}(\bar{\mathscr{I}}^i_{ps}+m_i(\|\boldsymbol{r}_i-\boldsymbol{r}_{\mathrm{cm}}\|^2\delta_{ps}-\hat{x}_{ip}\hat{x}_{is})), \tag{17}$$

where, for a spherical particle, $\bar{\mathscr{I}}^i_{pp}=\frac{2}{5}m_iR_i^2$, and for $p\neq s$, $\bar{\mathscr{I}}^i_{ps}=0$ (no products of inertia), R_i being the particle radius.[¶] Finally, for the derivative of the angular momentum, utilizing $\ddot{\boldsymbol{r}}_i=\boldsymbol{a}_i=\boldsymbol{a}_{\mathrm{cm}}+\boldsymbol{a}_{\mathrm{cm}\to i}$, we obtain

$$\dot{\boldsymbol{H}}^{\mathrm{rel}}_{\mathrm{cm}}=\sum_{i=1}^{N_c}(\boldsymbol{r}_{\mathrm{cm}\to i}\times m_i\boldsymbol{a}_{\mathrm{cm}\to i})=\sum_{i=1}^{N_c}(\boldsymbol{r}_{\mathrm{cm}\to i}\times m_i(\boldsymbol{a}_i-\boldsymbol{a}_{\mathrm{cm}})) \tag{18}$$

$$=\sum_{i=1}^{N_c}(m_i\boldsymbol{r}_{\mathrm{cm}\to i}\times\boldsymbol{a}_i)-\underbrace{\left(\sum_{i=1}^{N_c}m_i\boldsymbol{r}_{\mathrm{cm}\to i}\right)}_{=0}\times\boldsymbol{a}_{\mathrm{cm}}=\dot{\boldsymbol{H}}_{\mathrm{cm}}, \tag{19}$$

and consequently

$$\dot{\boldsymbol{H}}_{\mathrm{cm}}=\frac{\mathrm{d}(\overline{\boldsymbol{I}}\cdot\boldsymbol{\omega})}{\mathrm{d}t}=\sum_{i=1}^{N_c}\boldsymbol{r}_{\mathrm{cm}\to i}\times\boldsymbol{\psi}_i^{\mathrm{ext}}=\sum_{i=1}^{N_c}\boldsymbol{r}_{\mathrm{cm}\to i}\times q_i(\boldsymbol{E}^{\mathrm{ext}}+\boldsymbol{v}_i\times\boldsymbol{B}^{\mathrm{ext}})\overset{\mathrm{def}}{=}\boldsymbol{M}^{\mathrm{EXT}}_{\mathrm{cm}}, \tag{20}$$

where $\boldsymbol{M}^{\mathrm{EXT}}_{\mathrm{cm}}$ is the total external moment about the center-of-mass.

3. DECOMPOSITION OF THE ELECTROMAGNETIC CONTRIBUTIONS

Consider a rigid cluster of charged particles with angular velocity $\boldsymbol{\omega}$ and center-of-mass velocity $\boldsymbol{v}_{\mathrm{cm}}$.

[¶] If the particles are sufficiently small, each particle's own moment inertia (about its own center) is insignificant, leading to $\bar{I}_{ps}=\sum_{i=1}^{N_c}m_i(\|\boldsymbol{r}_i-\boldsymbol{r}_{\mathrm{cm}}\|^2\delta_{ps}-\hat{x}_{ip}\hat{x}_{is})$.

DOI: 10.1002/nme

3.1. The overall forces and moments

The velocity of any point on the body can be represented by

$$\boldsymbol{v}_i = \boldsymbol{v}_{\rm cm} + \boldsymbol{\omega} \times \boldsymbol{r}_{{\rm cm}\to i}, \tag{21}$$

and the overall external electromagnetic force $\boldsymbol{\Psi}^{\rm EXT} = \sum_{i=1}^{N_{\rm c}} q_i (\boldsymbol{E}^{\rm ext} + \boldsymbol{v} \times \boldsymbol{B}^{\rm ext})$ can be decomposed into the following parts:

$$\begin{aligned}\boldsymbol{\Psi}^{\rm EXT} = & \underbrace{\sum_{i=1}^{N_{\rm c}} q_i \boldsymbol{E}^{\rm ext}}_{\text{electrical contribution}} + \underbrace{\sum_{i=1}^{N_{\rm c}} q_i (\boldsymbol{v}_{\rm cm} \times \boldsymbol{B}^{\rm ext})}_{\text{linear velocity contribution}} + \underbrace{\sum_{i=1}^{N_{\rm c}} q_i ((\boldsymbol{\omega} \times \boldsymbol{r}_{{\rm cm}\to i}) \times \boldsymbol{B}^{\rm ext})}_{\text{angular velocity contribution}} \\ = & \boldsymbol{E}^{\rm ext} \left(\sum_{i=1}^{N_{\rm c}} q_i \right) + \boldsymbol{v}_{\rm cm} \times \boldsymbol{B}^{\rm ext} \left(\sum_{i=1}^{N_{\rm c}} q_i \right) + \boldsymbol{\omega} \times \left(\sum_{i=1}^{N_{\rm c}} q_i \times \boldsymbol{r}_{{\rm cm}\to i} \right) \times \boldsymbol{B}^{\rm ext}, \end{aligned} \tag{22}$$

and, similarly, for the total external moment about the center-of-mass

$$\begin{aligned}\boldsymbol{M}_{\rm cm}^{\rm EXT} = & \sum_{i=1}^{N_{\rm c}} \boldsymbol{r}_{{\rm cm}\to i} \times \left(\underbrace{q_i \boldsymbol{E}^{\rm ext}}_{\text{electrical contribution}} + \underbrace{q_i (\boldsymbol{v}_{\rm cm} \times \boldsymbol{B}^{\rm ext})}_{\text{linear velocity contribution}} + \underbrace{q_i ((\boldsymbol{\omega} \times \boldsymbol{r}_{{\rm cm}\to i}) \times \boldsymbol{B}^{\rm ext})}_{\text{angular velocity contribution}} \right) \\ = & \left(\sum_{i=1}^{N_{\rm c}} q_i \boldsymbol{r}_{{\rm cm}\to i} \right) \times \boldsymbol{E}^{\rm ext} + \left(\sum_{i=1}^{N_{\rm c}} q_i \boldsymbol{r}_{{\rm cm}\to i} \right) \times \boldsymbol{v}_{\rm cm} \times \boldsymbol{B}^{\rm ext} + \left(\sum_{i=1}^{N_{\rm c}} q_i \boldsymbol{r}_{{\rm cm}\to i} \times \boldsymbol{\omega} \times \boldsymbol{r}_{{\rm cm}\to i} \right) \times \boldsymbol{B}^{\rm ext} \\ = & \boldsymbol{R}_q \times \boldsymbol{E}^{\rm ext} + \boldsymbol{R}_q \times \boldsymbol{v}_{\rm cm} \times \boldsymbol{B}^{\rm ext} + \boldsymbol{H}_q \times \boldsymbol{B}^{\rm ext}, \end{aligned} \tag{23}$$

where

- $\boldsymbol{R}_q \stackrel{\rm def}{=} \sum_{i=1}^{N_{\rm c}} q_i \boldsymbol{r}_{{\rm cm}\to i}$ is defined as the *center of charge relative to the center-of-mass* and
- $\boldsymbol{H}_q \stackrel{\rm def}{=} \sum_{i=1}^{N_{\rm c}} q_i \boldsymbol{H}_{{\rm cm}\to i}/m_i$ is defined as the *charged angular momentum per unit mass with respect to the center-of-mass.*

Thus, the following three quantities play a central role in the cluster behavior:

- the sum of the individual charges ('overall charge'/first moment): $Q \stackrel{\rm def}{=} \sum_{i=1}^{N_{\rm c}} q_i$,
- the sum of the distances between the individual charged particles ($\boldsymbol{r}_i$) and the center-of-mass of the cluster ($\boldsymbol{r}_{\rm cm}$), weighted by the individual charges ('charged radius'/second-moment): $\boldsymbol{R}_q \stackrel{\rm def}{=} \sum_{i=1}^{N_{\rm c}} q_i (\boldsymbol{r}_i - \boldsymbol{r}_{\rm cm})$ and
- the sum of the self-cross-product of the distances between the individual charged particles and the center-of-mass of the cluster, weighted by the individual charges ($\bar{\boldsymbol{I}}_q$, 'moment of charge'/third-moment): $\boldsymbol{H}_q = \bar{\boldsymbol{I}}_q \cdot \boldsymbol{\omega} \stackrel{\rm def}{=} \sum_{i=1}^{N_{\rm c}} q_i (\boldsymbol{r}_i - \boldsymbol{r}_{\rm cm}) \times \boldsymbol{\omega} \times (\boldsymbol{r}_i - \boldsymbol{r}_{\rm cm})$, where $\boldsymbol{\omega}$ is the angular velocity of the body and where $\bar{\boldsymbol{I}}_q$ has components $(p, s = 1, 2, 3)$

$$\bar{I}_{q,ps} = \sum_{i=1}^{N_{\rm c}} q_i (\|\boldsymbol{r}_i - \boldsymbol{r}_{\rm cm}\|^2 \delta_{ps} - \hat{x}_{ip} \hat{x}_{is}). \tag{24}$$

DOI: 10.1002/nme

3.2. Various charge distribution cases

In summary, for a charged cluster, the governing equations may be written as

$$\mathscr{M}\ddot{\boldsymbol{r}}_{\mathrm{cm}} = \mathscr{M}\dot{\boldsymbol{v}}_{\mathrm{cm}} = \boldsymbol{\Psi}^{\mathrm{EXT}} = \underbrace{Q\boldsymbol{E}^{\mathrm{ext}}}_{\mathscr{T}_1} + \underbrace{Q\boldsymbol{v}_{\mathrm{cm}} \times \boldsymbol{B}^{\mathrm{ext}}}_{\mathscr{T}_2} + \underbrace{(\boldsymbol{\omega} \times \boldsymbol{R}_q) \times \boldsymbol{B}^{\mathrm{ext}}}_{\mathscr{T}_3}, \tag{25}$$

and

$$\dot{\boldsymbol{H}}_{\mathrm{cm}} = \frac{\mathrm{d}(\bar{\boldsymbol{I}} \cdot \boldsymbol{\omega})}{\mathrm{d}t} = \boldsymbol{M}_{\mathrm{cm}}^{\mathrm{EXT}} = \underbrace{\boldsymbol{R}_q \times \boldsymbol{E}^{\mathrm{ext}}}_{\mathscr{T}_4} + \underbrace{\boldsymbol{R}_q \times \boldsymbol{v}_{\mathrm{cm}} \times \boldsymbol{B}^{\mathrm{ext}}}_{\mathscr{T}_5} + \underbrace{(\bar{\boldsymbol{I}}_q \cdot \boldsymbol{\omega}) \times \boldsymbol{B}^{\mathrm{ext}}}_{\mathscr{T}_6}. \tag{26}$$

One may observe that

- in the special case when the overall charge (Q) of the cluster is zero (neutral), $\mathscr{T}_1 = \mathscr{T}_2 = 0$,
- in the special case when the overall charged distances ($\boldsymbol{R}_q$) are evenly distributed with respect to the mass-center, $\mathscr{T}_3 = \mathscr{T}_4 = \mathscr{T}_5 = 0$ and
- in the special case when the overall charged moment ($\bar{\boldsymbol{I}}_q$) is zero, $\mathscr{T}_6 = 0$.

Also, one has

$$\begin{aligned} \|\boldsymbol{\Psi}^{\mathrm{EXT}}\| &= \|Q(\boldsymbol{E}^{\mathrm{ext}} + \boldsymbol{v}_{\mathrm{cm}} \times \boldsymbol{B}^{\mathrm{ext}}) + (\boldsymbol{\omega} \times \boldsymbol{R}_q) \times \boldsymbol{B}^{\mathrm{ext}}\| \\ &\leqslant |Q| \|\boldsymbol{E}^{\mathrm{ext}} + \boldsymbol{v}_{\mathrm{cm}} \times \boldsymbol{B}^{\mathrm{ext}}\| + \|\boldsymbol{R}_q\| \|\boldsymbol{\omega}\| \|\boldsymbol{B}^{\mathrm{ext}}\| \\ &\leqslant |Q| \|\boldsymbol{E}^{\mathrm{ext}}\| + |Q| \|\boldsymbol{v}_{\mathrm{cm}}\| \|\boldsymbol{B}^{\mathrm{ext}}\| + \|\boldsymbol{R}_q\| \|\boldsymbol{\omega}\| \|\boldsymbol{B}^{\mathrm{ext}}\| \end{aligned} \tag{27}$$

and

$$\begin{aligned} \|\boldsymbol{M}_{\mathrm{cm}}^{\mathrm{EXT}}\| &= \|\boldsymbol{R}_q \times (\boldsymbol{E}^{\mathrm{ext}} + \boldsymbol{v}_{\mathrm{cm}} \times \boldsymbol{B}^{\mathrm{ext}}) + (\bar{\boldsymbol{I}}_q \cdot \boldsymbol{\omega}) \times \boldsymbol{B}^{\mathrm{ext}}\| \\ &\leqslant \|\boldsymbol{R}_q\| \|\boldsymbol{E}^{\mathrm{ext}} + \boldsymbol{v}_{\mathrm{cm}} \times \boldsymbol{B}^{\mathrm{ext}}\| + \|\bar{\boldsymbol{I}}_q\| \|\boldsymbol{\omega}\| \|\boldsymbol{B}^{\mathrm{ext}}\| \\ &\leqslant \|\boldsymbol{R}_q\| \|\boldsymbol{E}^{\mathrm{ext}}\| + \|\boldsymbol{R}_q\| \|\boldsymbol{v}_{\mathrm{cm}}\| \end{aligned} \tag{28}$$

Thus, both Q and $\|\boldsymbol{R}_q\|$ must be zero for $\|\boldsymbol{\Psi}^{\mathrm{EXT}}\| = 0$, whereas both $\|\boldsymbol{R}_q\|$ and $\|\bar{\boldsymbol{I}}_q\|$ must be zero for $\|\boldsymbol{M}_{\mathrm{cm}}^{\mathrm{EXT}}\| = 0$. Clearly, each of the (zero/non-zero) cases can occur independently of one another.

Remark
The dynamics of a general cluster must be treated numerically, particularly when one has a three-dimensional body with a complex charge distribution. This is discussed next.

4. NUMERICAL METHODS FOR THE DYNAMICS OF A CHARGED CLUSTER

We now treat the dynamics of a cluster numerically. We first focus on the translational motion of the center-of-mass, and then turn to the rotational contribution.

DOI: 10.1002/nme

4.1. Cluster translational contribution

The translational component of the center-of-mass can be written as

$$\mathscr{M}\ddot{\boldsymbol{r}}_{\rm cm}=\mathscr{M}\dot{\boldsymbol{v}}_{\rm cm}=\boldsymbol{\Psi}^{\rm EXT}. \tag{29}$$

A trapezoidal-rule is used (see Appendix), whereby at some intermediate moment in time $t\leqslant t+\phi\Delta t\leqslant t+\Delta t$ $(0\leqslant\phi\leqslant 1)$

$$\begin{aligned}\dot{\boldsymbol{v}}_{\rm cm}(t+\phi\Delta t)&\approx\frac{\boldsymbol{v}_{\rm cm}(t+\Delta t)-\boldsymbol{v}_{\rm cm}(t)}{\Delta t}=\frac{1}{\mathscr{M}}\boldsymbol{\Psi}^{\rm EXT}(t+\phi\Delta t)\\&\approx\frac{1}{\mathscr{M}}(\phi\boldsymbol{\Psi}^{\rm EXT}(t+\Delta t)+(1-\phi)\boldsymbol{\Psi}^{\rm EXT}(t)),\end{aligned} \tag{30}$$

leading to

$$\boldsymbol{v}_{\rm cm}(t+\Delta t)=\boldsymbol{v}_{\rm cm}(t)+\frac{\Delta t}{\mathscr{M}}(\phi\boldsymbol{\Psi}^{\rm EXT}(t+\Delta t)+(1-\phi)\boldsymbol{\Psi}^{\rm EXT}(t)). \tag{31}$$

For the position, we have

$$\dot{\boldsymbol{r}}_{\rm cm}(t+\phi\Delta t)\approx\frac{\boldsymbol{r}_{\rm cm}(t+\Delta t)-\boldsymbol{r}_{\rm cm}(t)}{\Delta t}\approx\boldsymbol{v}_{\rm cm}(t+\phi\Delta t)\approx(\phi\boldsymbol{v}_{\rm cm}(t+\Delta t)+(1-\phi)\boldsymbol{v}_{\rm cm}(t)), \tag{32}$$

leading to

$$\boldsymbol{r}_{\rm cm}(t+\Delta t)=\boldsymbol{r}_{\rm cm}(t)+\Delta t(\phi\boldsymbol{v}_{\rm cm}(t+\Delta t)+(1-\phi)\boldsymbol{v}_{\rm cm}(t)). \tag{33}$$

Remark
More details on the time-stepping schemes are provided in the Appendix.

4.2. Cluster rotational motion

There are two possible approaches to compute the cluster rotations, either using a (1) inertially fixed frame or (2) body-fixed frame. We employ an inertially fixed approach, and implicit time-stepping, for the duration of the presentation. This straightforward approach entails, at each (implicit) time-step, decomposing an increment of motion into an incremental rigid-body translational contribution and an incremental rigid-body rotational contribution (rotation about the center-of-mass). The rotational contribution is determined by solving a set of coupled nonlinear equations governing the angular velocity and the incremental rotation of the body around the axis of rotation (which also changes as a function of time). The equation for the angular momentum can be written as

$$\dot{\boldsymbol{H}}_{\rm cm}=\frac{{\rm d}(\bar{\boldsymbol{I}}\cdot\boldsymbol{\omega})}{{\rm d}t}=\boldsymbol{M}^{\rm EXT}_{\rm cm}. \tag{34}$$

Because the body rotates, $\bar{\boldsymbol{I}}$ is implicitly dependent on $\boldsymbol{\omega}$ (and hence time), which leads to a coupled system of nonlinear ODE's, which can be solved with an iterative scheme. Equation (34) is discretized by a trapezoidal scheme (as for the translational component)

$$\left.\frac{{\rm d}(\bar{\boldsymbol{I}}\cdot\boldsymbol{\omega})}{{\rm d}t}\right|_{t+\phi\Delta t}=\frac{(\bar{\boldsymbol{I}}\cdot\boldsymbol{\omega})|_{t+\Delta t}-(\bar{\boldsymbol{I}}\cdot\boldsymbol{\omega})|_{t}}{\Delta t}, \tag{35}$$

DOI: 10.1002/nme

thus leading to

$$(\bar{\boldsymbol{I}}\cdot\boldsymbol{\omega})|_{t+\Delta t}=(\bar{\boldsymbol{I}}\cdot\boldsymbol{\omega})|_t+\Delta t\boldsymbol{M}_{\mathrm{cm}}^{\mathrm{EXT}}(t+\phi\Delta t). \tag{36}$$

Solving for $\boldsymbol{\omega}(t+\Delta t)$ yields

$$\boldsymbol{\omega}(t+\Delta t)=(\bar{\boldsymbol{I}}(t+\Delta t))^{-1}\cdot((\bar{\boldsymbol{I}}\cdot\boldsymbol{\omega})|_t+\Delta t\boldsymbol{M}_{\mathrm{cm}}^{\mathrm{EXT}}(t+\phi\Delta t)), \tag{37}$$

where

$$\boldsymbol{M}_{\mathrm{cm}}^{\mathrm{EXT}}(t+\phi\Delta t)\approx\phi\boldsymbol{M}_{\mathrm{cm}}^{\mathrm{EXT}}(t+\Delta t)+(1-\phi)\boldsymbol{M}_{\mathrm{cm}}^{\mathrm{EXT}}(t), \tag{38}$$

which yields an implicit nonlinear equation, of the form $\boldsymbol{\omega}(t+\Delta t)=\mathscr{F}(\boldsymbol{\omega}(t+\Delta t))$, since $\bar{\boldsymbol{I}}(t+\Delta t)$, due to the body's rotation. An iterative, implicit, solution scheme may be written as follows (for iterations $K=1,2,\ldots$):

$$\boldsymbol{\omega}^{K+1}(t+\Delta t)=(\bar{\boldsymbol{I}}^{K}(t+\Delta t))^{-1}\cdot((\bar{\boldsymbol{I}}\cdot\boldsymbol{\omega})|_t+\Delta t\boldsymbol{M}_{\mathrm{cm}}^{\mathrm{EXT},K}(t+\phi\Delta t)), \tag{39}$$

where $\bar{\boldsymbol{I}}^{K}(t+\Delta t)$ can be computed by a similarity transform (described shortly).[‖] After the update for $\boldsymbol{\omega}^{K+1}(t+\Delta t)$ has been computed (utilizing the $\bar{\boldsymbol{I}}^{K}(t+\Delta t)$ from the previous iteration), the rotation of the body about the center-of-mass can be determined. The *incremental* angular rotation around the instantaneous rotation axis $\boldsymbol{a}^{K+1}(t+\phi\Delta t)$ (which will also have to be updated) is obtained by $(\boldsymbol{\omega}^{K+1}(t+\phi\Delta t)=\omega^{K+1}(t+\phi\Delta t)\boldsymbol{a}^{K+1}(t+\phi\Delta t))$

$$\frac{\mathrm{d}\theta^{K+1}}{\mathrm{d}t}(t+\phi\Delta t)=\omega^{K+1}(t+\phi\Delta t)\approx\frac{\Delta\theta^{K+1}(t+\phi\Delta t)}{\Delta t}, \tag{40}$$

where $\omega^{K+1}(t+\phi\Delta t)=\|\boldsymbol{\omega}^{K+1}(t+\phi\Delta t)\|$ is *a scalar* rotation about the instantaneous axis,

$$\boldsymbol{a}^{K+1}(t+\phi\Delta t)\overset{\mathrm{def}}{=}\frac{\boldsymbol{\omega}^{K+1}(t+\phi\Delta t)}{\|\boldsymbol{\omega}^{K+1}(t+\phi\Delta t)\|}\approx\frac{\phi\boldsymbol{\omega}^{K+1}(t+\Delta t)+(1-\phi)\boldsymbol{\omega}(t)}{\|\phi\boldsymbol{\omega}^{K+1}(t+\Delta t)+(1-\phi)\boldsymbol{\omega}(t)\|}, \tag{41}$$

and thus

$$\Delta\theta^{K+1}(t+\phi\Delta t)=\omega^{K+1}(t+\phi\Delta t)\Delta t, \tag{42}$$

where $\omega^{K+1}(t+\Delta t)=\|\phi\boldsymbol{\omega}^{K+1}(t+\Delta t)+(1-\phi)\boldsymbol{\omega}(t)\|$. To determine the movement of the individual points/particles in the rigid (cluster) body, we need to perform a rigid-body translation and rotation (described in the next section). For example, consider a point $\boldsymbol{r}_i$ on the body. The update would be

$$\boldsymbol{r}_i(t+\Delta t)=\boldsymbol{r}_i(t)+\underbrace{\boldsymbol{u}_{\mathrm{cm}}}_{\text{due to cm translation}}+\underbrace{\boldsymbol{u}_{i,\mathrm{rot}}}_{\text{due to rotation w.r.t. cm}} \tag{43}$$

where

$$\boldsymbol{u}_{\mathrm{cm}}=\boldsymbol{r}_{\mathrm{cm}}(t+\Delta t)-\boldsymbol{r}_{\mathrm{cm}}(t) \tag{44}$$

[‖]One may view the overall process as a fixed-point calculation of the form $\boldsymbol{\omega}^{K+1}(t+\Delta t)=\mathscr{F}(\boldsymbol{\omega}^{K}(t+\Delta t))$.

DOI: 10.1002/nme

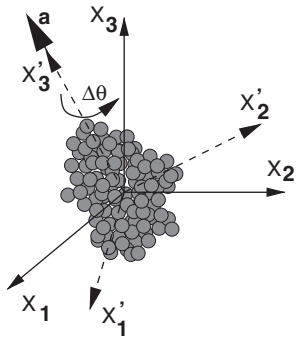

Figure 3. Aligning the primed coordinate system with the instantaneous axis of rotation ($\boldsymbol{a}$) for a cluster.

and $\boldsymbol{u}_{i,\mathrm{rot}}$ is the contribution due to an incremental rotation of the relative position vector

$$\boldsymbol{\tau}^{(i)} \stackrel{\mathrm{def}}{=} \boldsymbol{r}_i(t) - \boldsymbol{r}_{\mathrm{cm}}(t) \tag{45}$$

by $\Delta\theta$ about the center-of-mass (Figure 3).

4.3. Transformation matrices for updates and incremental rotation

In order to rotate any point i, with position vector $\boldsymbol{\tau}^{(i)}$, associated with the rigid body, we require some standard transformations. The same transformation is needed to rotate the body's moment of inertia, $\overline{\boldsymbol{I}}$ (Figure 3). It is a relatively standard exercise in linear algebra to show that any vector, $\boldsymbol{\tau}$, which can be expressed on either the unprimed or primed basis, $\boldsymbol{\tau} = (\boldsymbol{\tau}\cdot\boldsymbol{e}_i)\boldsymbol{e}_i = (\boldsymbol{\tau}\cdot\boldsymbol{e}'_j)\boldsymbol{e}'_j$, where the summation index notation is employed. These two representations are explicitly related by

$$\begin{bmatrix} \tau_1 \\ \tau_2 \\ \tau_3 \end{bmatrix}' = \underbrace{\begin{bmatrix} \boldsymbol{e}_1\cdot\boldsymbol{e}'_1 & \boldsymbol{e}_2\cdot\boldsymbol{e}'_1 & \boldsymbol{e}_3\cdot\boldsymbol{e}'_1 \\ \boldsymbol{e}_1\cdot\boldsymbol{e}'_2 & \boldsymbol{e}_2\cdot\boldsymbol{e}'_2 & \boldsymbol{e}_3\cdot\boldsymbol{e}'_2 \\ \boldsymbol{e}_1\cdot\boldsymbol{e}'_3 & \boldsymbol{e}_2\cdot\boldsymbol{e}'_3 & \boldsymbol{e}_3\cdot\boldsymbol{e}'_3 \end{bmatrix}}_{[\boldsymbol{A}]} \begin{bmatrix} \tau_1 \\ \tau_2 \\ \tau_3 \end{bmatrix}. \tag{46}$$

Note that $\boldsymbol{A}^{-1} = \boldsymbol{A}^{\mathrm{T}}$; thus, $\boldsymbol{\tau}' = \boldsymbol{A}\cdot\boldsymbol{\tau}$ and $\boldsymbol{\tau} = \boldsymbol{A}^{\mathrm{T}}\cdot\boldsymbol{\tau}'$. This basic result can be used to perform rotation of a vector about an axis, as well as the rotation of the inertia tensor. Without any loss of generality, we align the $\boldsymbol{e}'_3$ axis to instantaneous rotation axis $\boldsymbol{a}$. The total transformation (rotation) of a vector $\boldsymbol{\tau}^{(i)}$, representing a point i on the body, can be represented by

$$\underbrace{[\boldsymbol{\tau}^{(i)}]^{\mathrm{rot}}}_{[\boldsymbol{\tau}^{(i)}]^{\mathrm{rot}}} = \underbrace{[\boldsymbol{A}]^{\mathrm{T}}\,\underbrace{[\boldsymbol{R}(\Delta\theta)]\,\underbrace{[\boldsymbol{A}][\boldsymbol{\tau}_i]}_{[\boldsymbol{\tau}^{(i)}]'}}_{[\boldsymbol{\tau}^{(i)}]^{\mathrm{rot},\prime}}}_{[\boldsymbol{\tau}^{(i)}]^{\mathrm{rot}}}, \tag{47}$$

DOI: 10.1002/nme

where

$$[\boldsymbol{R}(\Delta\theta)]=\begin{bmatrix}\cos(\Delta\theta) & -\sin(\Delta\theta) & 0\\ \sin(\Delta\theta) & \cos(\Delta\theta) & 0\\ 0 & 0 & 1\end{bmatrix}. \tag{48}$$

Similarly, for the rotation inertia tensor

$$[\bar{\boldsymbol{I}}]^{\mathrm{rot}}=[\boldsymbol{A}]\,[\boldsymbol{R}(\Delta\theta)]^{\mathrm{T}}\underbrace{\underbrace{[\boldsymbol{A}]^{\mathrm{T}}[\bar{\boldsymbol{I}}][\boldsymbol{A}]}_{[\bar{\boldsymbol{I}}]'}}_{[\bar{\boldsymbol{I}}]^{\mathrm{rot},\prime}}[\boldsymbol{R}(\Delta\theta)][\boldsymbol{A}]^{\mathrm{T}}, \tag{49}$$

where, during the iterative calculations, $[\bar{\boldsymbol{I}}]=[\bar{\boldsymbol{I}}(t)]$ and $[\bar{\boldsymbol{I}}]^{\mathrm{rot}}=[\bar{\boldsymbol{I}}(t+\Delta t)]$.

4.4. Algorithmic procedure

The overall procedure is as follows, at time t:

1. Compute the new position of the center-of-mass.
2. Compute (iteratively) the incremental angular rotation of the body with respect to the center-of-mass until system convergence:

$$\|\boldsymbol{\omega}^{K+1}(t+\Delta t)-\boldsymbol{\omega}^{K}(t+\Delta t)\|\leqslant \mathrm{TOL}\|\boldsymbol{\omega}^{K+1}(t+\Delta t)\|. \tag{50}$$

   This requires a rotation of the body within the iterations:

   (a) Given that $\boldsymbol{\omega}^{K+1}(t+\Delta t)$ has been computed

$$\boldsymbol{\omega}^{K+1}(t+\Delta t)=(\bar{\boldsymbol{I}}^{K}(t+\Delta t))^{-1}\cdot((\bar{\boldsymbol{I}}\cdot\boldsymbol{\omega})|_{t}+\Delta t\boldsymbol{M}_{\mathrm{cm}}^{\mathrm{EXT},K}(t+\phi\Delta t)). \tag{51}$$

   (b) Compute the (updated) axis of rotation:

$$\boldsymbol{a}^{K+1}(t+\phi\Delta t)\overset{\mathrm{def}}{=}\frac{\boldsymbol{\omega}^{K+1}(t+\phi\Delta t)}{\|\boldsymbol{\omega}^{K+1}(t+\phi\Delta t)\|}\approx\frac{\phi\boldsymbol{\omega}^{K+1}(t+\Delta t)+(1-\phi)\boldsymbol{\omega}(t)}{\|\phi\boldsymbol{\omega}^{K+1}(t+\Delta t)+(1-\phi)\boldsymbol{\omega}(t)\|}. \tag{52}$$

   (c) Compute the basis $\boldsymbol{e}_3'$-aligned instantaneous axis of rotation ($\boldsymbol{a}$):

   (i) $\boldsymbol{e}_3'$ is aligned with $\boldsymbol{a}^{K+1}(t+\Delta t)$,
   (ii) $\boldsymbol{e}_1'=\boldsymbol{e}_3'\times\boldsymbol{e}_3/\|\boldsymbol{e}_3'\times\boldsymbol{e}_3\|$ and
   (iii) $\boldsymbol{e}_2'=\boldsymbol{e}_3'\times\boldsymbol{e}_1'/\|\boldsymbol{e}_3'\times\boldsymbol{e}_1'\|$.

   (d) Compute the composite transformation for the inertia tensor in Equation (49) and obtain the update $\bar{\boldsymbol{I}}^{K+1}(t+\Delta t)$.
   (e) Repeat steps (a)–(d) until Equation (50) is satisfied.
3. Compute the total new position of the points in the body (i) with Equation (47), increment time forward and repeat the procedure.

More details on the overall algorithm, including a general time-step adaptivity scheme, are given in the Appendix.

DOI: 10.1002/nme

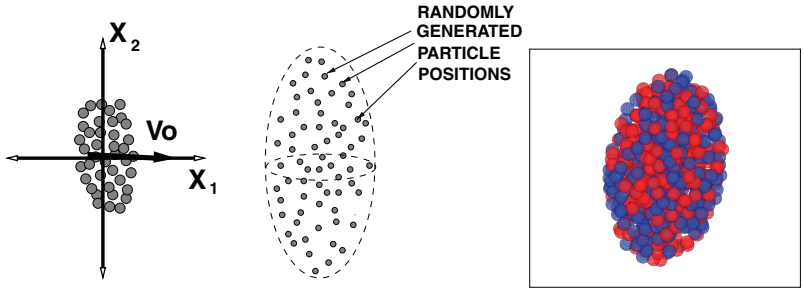

Figure 4. LEFT: the initial configuration; MIDDLE: an ellipsoidal envelope for the random particle positions; and RIGHT: the actual object used in computations (blue (online version) or black (print version) is a base-positive charge and red is a base-negative charge).

5. MODEL PROBLEMS/NUMERICAL EXAMPLES

As a model problem, we consider a cluster formed by randomly dispersing charged particulates within a prolate ellipsoidal domain (aspect ratio of 2:1, Figure 4). The radii of the ellipsoidal domain (envelope) in which the particles were randomly dispersed were 0.002 m (major axis) and 0.001 m (for both minor axes).** We considered $N_c = 500$ randomly distributed particles, with an overall charge of the body set to $\sum_{i=1}^{N_c} q_i = q^* = 0.01\,\mathrm{C}$, where $q_i = \pm q_o + q^*/N_c$. There were 250 base-positive ($q_o = +0.001$) and 250 base-negative ($q_o = -0.001$) particles in the system. The radii of the individual particles were set to $d = 0.0001\,\mathrm{m}$.††

In order to help investigate what type of motion a charged cluster will experience, we consider a 'comparison' case when only a single charged particle (or, considered equivalently, a lumped charged mass) is present in the system, with position vector denoted by $\boldsymbol{r}_s$, governed by Equation (1), written in a slightly different form here ($\dot{\boldsymbol{r}}_s = \boldsymbol{v}_s$)‡‡

$$m_s \ddot{\boldsymbol{r}}_s = q_s(\boldsymbol{E}^{\mathrm{ext}} + \dot{\boldsymbol{r}}_s \times \boldsymbol{B}^{\mathrm{ext}}). \tag{53}$$

The difference in the solution path for the single particle (governed by Equation (53)) and a multi-particle cluster, with center-of-mass given by $\boldsymbol{r}_{\mathrm{cm}}$ (governed by Equation (25) and implicitly by (26)) can be characterized by taking the difference between Equations (25) and (53) to obtain

$$\mathscr{M}\ddot{\boldsymbol{r}}_{\mathrm{cm}} - m\ddot{\boldsymbol{r}}_s = (Q - q_s)\boldsymbol{E}^{\mathrm{ext}} + (Q\dot{\boldsymbol{r}}_{\mathrm{cm}} - q_s\dot{\boldsymbol{r}}_s) \times \boldsymbol{B}^{\mathrm{ext}} + (\boldsymbol{\omega} \times \boldsymbol{R}_q \times \boldsymbol{B}^{\mathrm{ext}}). \tag{54}$$

**The absolute length-scales, charges and masses are somewhat irrelevant to the model problem framework, and can be scaled to any desired value for specific application.

††The densities for the particles were uniformly assigned $\rho = 2000$, with masses given by $m = \rho\frac{4}{3}\pi R^3$.

‡‡*Note*: The governing equation (53), written in a component form, is for component 1: $\dot{v}_{s1} = (q_s/m_s)(E_1^{\mathrm{ext}} + (v_{s2}B_3^{\mathrm{ext}} - v_{s3}B_2^{\mathrm{ext}}))$, for component 2: $\dot{v}_{s2} = (q_s/m_s)(E_2^{\mathrm{ext}} - (v_{s1}B_3^{\mathrm{ext}} - v_{s3}B_1^{\mathrm{ext}}))$ and for component 3: $\dot{v}_{s3} = (q_s/m_s)(E_3^{\mathrm{ext}} + (v_{s1}B_2^{\mathrm{ext}} - v_{s2}B_1^{\mathrm{ext}}))$. These equations can be solved analytically. There are a variety of possible particle trajectories, and we refer the reader to Jackson [36].

DOI: 10.1002/nme

If we assume $Q=q_s$, $M=m_s$ and define $\mathscr{E} \stackrel{\text{def}}{=} \boldsymbol{r}_{\text{cm}}-\boldsymbol{r}_s$, we obtain a 'deviation' equation governing the difference in the trajectories of the two systems

$$\ddot{\mathscr{E}}=\frac{1}{\mathscr{M}}(Q\dot{\mathscr{E}}\times\boldsymbol{B}^{\text{ext}}+\boldsymbol{\omega}\times\boldsymbol{R}_q\times\boldsymbol{B}^{\text{ext}}). \tag{55}$$

In the special case when $\boldsymbol{B}^{\text{ext}}=\boldsymbol{0}$, the difference between the motion of the center-of-mass is zero ($\mathscr{E}(t)=0$), although one can still expect rotation about the center-of-mass for the cluster, via $\boldsymbol{\omega}$, which is dictated by Equation (26).

5.1. *Special case # 1*: *no magnetic field* ($\boldsymbol{E}^{\text{ext}}\neq\boldsymbol{0}$ *and* $\boldsymbol{B}^{\text{ext}}=\boldsymbol{0}$)

In the special case when there is no magnetic field, if $\boldsymbol{r}_s(t=0)=\boldsymbol{0}$, $\boldsymbol{v}_s(t=0)=v_o\boldsymbol{e}_1$, $\boldsymbol{B}^{\text{ext}}=\boldsymbol{0}$ and $\boldsymbol{E}^{\text{ext}}=E^{\text{ext}}\boldsymbol{e}_3$, the solution for the dynamics of a single particle is

$$\begin{bmatrix} v_{s1}(t) \\ v_{s2}(t) \\ v_{s3}(t) \end{bmatrix} = \begin{bmatrix} v_o \\ 0 \\ \dfrac{q_s}{m_s}E_3^{\text{ext}}t \end{bmatrix} \Rightarrow \begin{bmatrix} r_{s1}(t) \\ r_{s2}(t) \\ r_{s3}(t) \end{bmatrix} = \begin{bmatrix} v_o t \\ 0 \\ \dfrac{q_s}{2m_s}E_3^{\text{ext}}t^2 \end{bmatrix}. \tag{56}$$

Now, for a cluster,[§§] let us (numerically) consider this special case ($\boldsymbol{v}(t=0)=0.01\boldsymbol{e}_1$, $\boldsymbol{\omega}(t=0)=\boldsymbol{0}$, $\boldsymbol{B}^{\text{ext}}=\boldsymbol{0}$ and $\boldsymbol{E}^{\text{ext}}=0.1\boldsymbol{e}_3$), which should yield results similar to a single particle in Equation (56). Indeed, as shown in Figure 5, as in the single particle case, when $\boldsymbol{B}^{\text{ext}}=\boldsymbol{0}$, we have the predicted motion, i.e. the center-of-mass of a cluster behaves similar to that of a single particle. However, notice in Figure 6, because of the term $\mathscr{T}_4\neq 0$ in Equation (26), there is rotational motion about the center-of-mass. This rotation (a twisting back and forth) about the center-of-mass is purely induced by the electric field. We emphasize, for this special case, because the only 'forcing term' on the right-hand side of the angular momentum Equation (26) is $\mathscr{T}_4 \stackrel{\text{def}}{=} \boldsymbol{R}_q\times\boldsymbol{E}^{\text{ext}}$ (since $\boldsymbol{B}^{\text{ext}}=\boldsymbol{0}$); $\boldsymbol{E}^{\text{ext}}$ is solely responsible for any spin of the cluster about its mass-center. This term manifests the oscillations seen in Figure 6 and is a phenomenon that is nonexistent in the single particle solution Equation (56).

5.2. *Special case # 2*: *no electric field* ($\boldsymbol{E}^{\text{ext}}=\boldsymbol{0}$ *and* $\boldsymbol{B}^{\text{ext}}\neq\boldsymbol{0}$)

Now consider a case with no electric field and a magnetic field present, $\boldsymbol{r}_s(t=0)=\boldsymbol{0}$, $\boldsymbol{v}_s(t=0)=v_o\boldsymbol{e}_1$, $\boldsymbol{B}^{\text{ext}}=B_3^{\text{ext}}\boldsymbol{e}_3$ and $\boldsymbol{E}^{\text{ext}}=\boldsymbol{0}$. Consequently, for a single particle, the solution is

$$\begin{bmatrix} v_{s1}(t) \\ v_{s2}(t) \\ v_{s3}(t) \end{bmatrix} = \begin{bmatrix} v_o\cos\Omega_s t \\ -v_o\sin\Omega_s t \\ 0 \end{bmatrix} \Rightarrow \begin{bmatrix} r_{s1}(t) \\ r_{s2}(t) \\ r_{s3}(t) \end{bmatrix} = \begin{bmatrix} \dfrac{v_o}{\Omega_s}\sin\Omega_s t \\ \dfrac{v_o}{\Omega_s}(\cos\Omega_s t-1) \\ 0 \end{bmatrix}, \tag{57}$$

[§§] These specific parameter choices resulted in $\|\boldsymbol{R}_q\|=0.00297$ and $\|\bar{\boldsymbol{I}}_q\|=0.0000229$. The simulations were run for other large clusters with similar trends occurring. In other words, these results are representative. The overall approach is general, and is valid for any distribution of charges.

DOI: 10.1002/nme

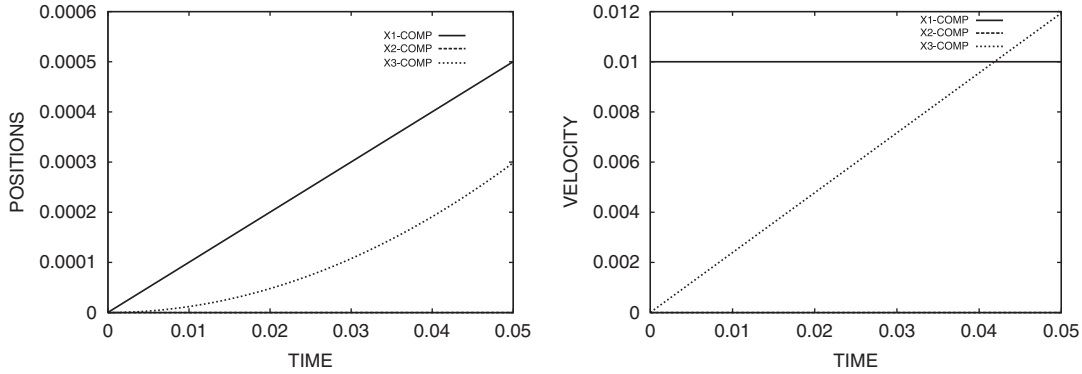

Figure 5. Special case 1: $\boldsymbol{v}(t=0)=0.01\boldsymbol{e}_1$, $\boldsymbol{B}^{\text{ext}}=\boldsymbol{0}$ and $\boldsymbol{E}^{\text{ext}}=0.1\boldsymbol{e}_3$. LEFT: the position of the center-of–mass. RIGHT: the velocity of the center-of-mass. The trajectory of the center-of-mass of the cluster is similar to that of a single charged particle.

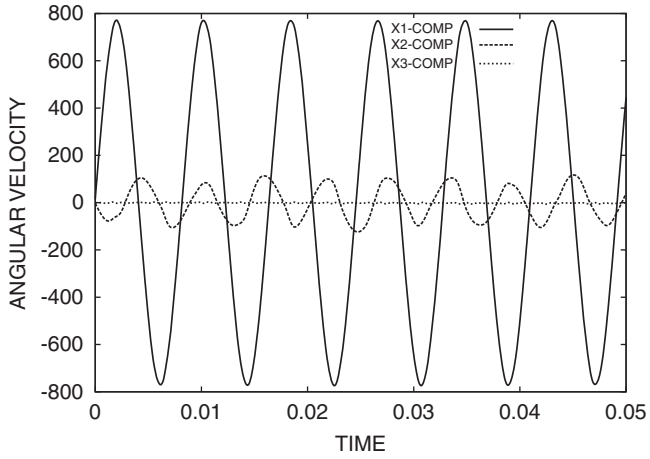

Figure 6. Special case 1: $\boldsymbol{v}(t=0)=0.01\boldsymbol{e}_1$, $\boldsymbol{B}^{\text{ext}}=\boldsymbol{0}$ and $\boldsymbol{E}^{\text{ext}}=0.1\boldsymbol{e}_3$: the angular velocity. The rotation about the center-of-mass is induced entirely by the electric field.

where $\Omega_s=q_sB_3^{\text{ext}}/m_s$ is known as the cyclotron frequency. The cyclotron frequency (gyrofrequency) is the angular frequency at which a charged particle makes circular orbits in a plane perpendicular to the static magnetic field. Notice that when $E_3^{\text{ext}}=0$, this traces out the equation of a circle centered at $(0,-v_o/\Omega_s)$. The radius of the 'magnetically induced circle' (radius of oscillation) is[¶¶]

$$\mathscr{R}\overset{\text{def}}{=}\frac{v_o}{\Omega_s}=\frac{v_om_s}{q_sB_3^{\text{ext}}}. \tag{58}$$

[¶¶]This field generates helical motion in three dimensions when $\boldsymbol{E}^{\text{ext}}\neq\boldsymbol{0}$.

DOI: 10.1002/nme

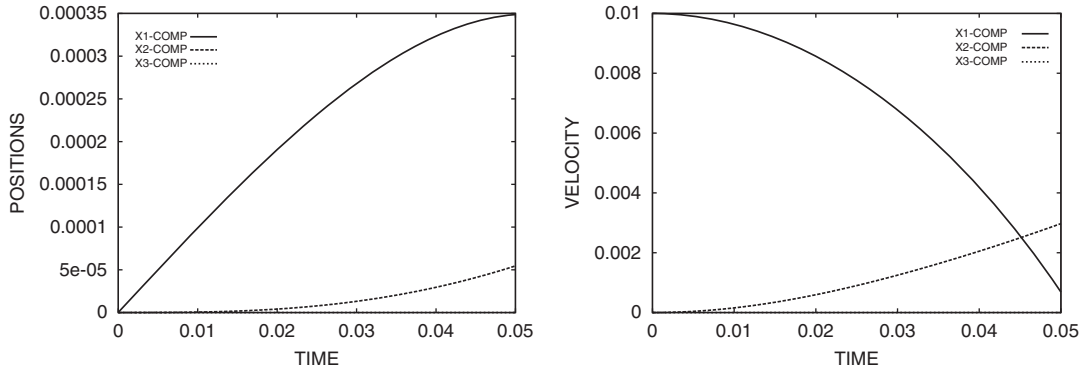

Figure 7. Special case 2: $\boldsymbol{v}(t=0)=0.01\boldsymbol{e}_1$, $\boldsymbol{B}^{\text{ext}}=0.01\boldsymbol{e}_3$ and $\boldsymbol{E}^{\text{ext}}=\boldsymbol{0}$. LEFT: the position of the center-of–mass. RIGHT: the velocity of the center-of-mass.

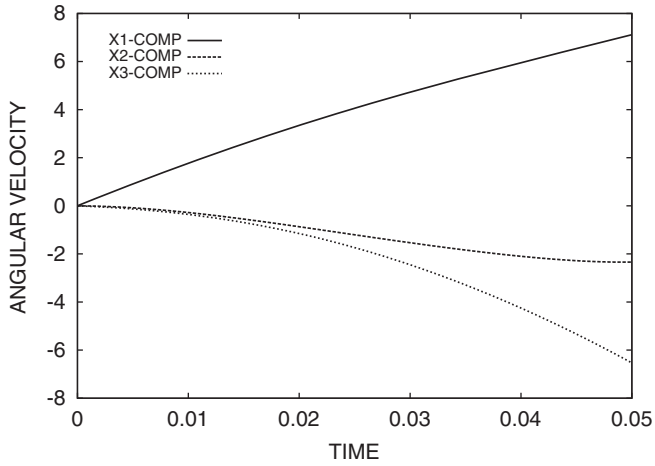

Figure 8. Special case 2: $\boldsymbol{v}(t=0)=0.01\boldsymbol{e}_1$, $\boldsymbol{B}^{\text{ext}}=0.01\boldsymbol{e}_3$ and $\boldsymbol{E}^{\text{ext}}=\boldsymbol{0}$: the angular velocity.

Thus, if a desired 'turning radius' is denoted by $\mathscr{R}$, one may solve for the magnetic field that delivers the desired effect, $B_3^{\text{ext}}=v_o m_s/(q_s\mathscr{R})$. We define the corresponding time period for one cycle to be completed as $T\stackrel{\text{def}}{=}2\pi/\Omega_s$. For the parameters chosen, this results in $\mathscr{R}=0.0004188\,\text{m}$, $\Omega_s=23.87\,\text{rad/s}$ and $T=0.1315\,\text{s}$. For a cluster (numerically computed with an initial $\boldsymbol{\omega}(t=0)$), Figure 7 illustrates motion with a possible long-range period T and 'large-scale' turning (cyclotron) radius ($\mathscr{R}$) that is similar to that of a single particle.[|||] Figure 8 indicates that there is some slight rotation of the body around the center-of-mass.

[|||]Figure 7 illustrates approximately one-quarter of a period (total period $T\approx 20\,\text{s}$) and a cyclotron radius of $\mathscr{R}\approx 0.0004\,\text{m}$.

DOI: 10.1002/nme

5.3. General case # 3: combined electric and magnetic fields ($\boldsymbol{E}^{\text{ext}} \neq \boldsymbol{0}$ *and* $\boldsymbol{B}^{\text{ext}} \neq \boldsymbol{0}$)

Now consider both the electric and magnetic fields to be present, $\boldsymbol{r}_s(t=0)=\boldsymbol{0}$, $\boldsymbol{v}_s(t=0)=v_o\boldsymbol{e}_1$, $\boldsymbol{B}^{\text{ext}}=B_3^{\text{ext}}\boldsymbol{e}_3$ and $\boldsymbol{E}^{\text{ext}}=E_3^{\text{ext}}\boldsymbol{e}_3$; consequently, for a single particle

$$\begin{bmatrix} v_{s1}(t) \\ v_{s2}(t) \\ v_{s3}(t) \end{bmatrix} = \begin{bmatrix} v_o \cos\Omega_s t \\ -v_o \sin\Omega_s t \\ \dfrac{q_s}{m_s} E_3^{\text{ext}} t \end{bmatrix} \Rightarrow \begin{bmatrix} r_{s1}(t) \\ r_{s2}(t) \\ r_{s3}(t) \end{bmatrix} = \begin{bmatrix} \dfrac{v_o}{\Omega_s} \sin\Omega_s t \\ \dfrac{v_o}{\Omega_s}(\cos\Omega_s t - 1) \\ \dfrac{q_s}{2m_s} E_3^{\text{ext}} t^2 \end{bmatrix}. \tag{59}$$

Let us now consider these parameters for a cluster ($\boldsymbol{r}(t=0)=\boldsymbol{0}$, $\boldsymbol{\omega}(t=0)=\boldsymbol{0}$, $\boldsymbol{v}(t=0)=0.01\boldsymbol{e}_1$, $\boldsymbol{B}^{\text{ext}}=0.01\boldsymbol{e}_3$ and $\boldsymbol{E}^{\text{ext}}=0.1\boldsymbol{e}_3$). As shown in Figure 7, there is large-scale reversal of the x_1 component with a superposed oscillatory 'wobble'. As in special case #2, there would be large-scale turning of the cluster, albeit slowly induced, due to a (nonmonotonic) reversal of the x_1 velocity, which would eventually trace out a helix-like path in the x_1–x_2 plane moving upwards in the x_3 direction. The rotations about the center-of-mass are highly variable due to the random positions of the charged particles within the cluster. Figure 9 indicates the dramatic difference (due to the absence of the electric field) between special case # 2 and general case # 3 (Figure 10), which is predicted by Equation (55). The key observation is that the effects of $\boldsymbol{E}^{\text{ext}}$ and $\boldsymbol{B}^{\text{ext}}$ are strongly coupled via Equations (25) and (26), as opposed to uncoupled (as exhibited by Equations (57) and (59)). One reason for this strong coupling is due to the dependence of $\boldsymbol{\omega}$ on $\boldsymbol{E}^{\text{ext}}$, as exhibited by Equation (26). Even when $Q=q_s=0$, the trajectory deviation is governed by

$$\ddot{\boldsymbol{\mathscr{E}}} = \frac{1}{\mathscr{M}}(\boldsymbol{\omega} \times \boldsymbol{R}_q \times \boldsymbol{B}^{\text{ext}}), \tag{60}$$

and is strongly influenced by a balance of angular momentum, through $\boldsymbol{\omega}$, which is governed by Equation (26). The influence of $\boldsymbol{E}^{\text{ext}}$ comes through Equation (26), via term $\mathscr{T}_4$, even when $Q=0$. We further note that in the special case when $\boldsymbol{R}_q=\boldsymbol{0}$ and $Q=q_s\neq 0$, the deviation is governed by

$$\ddot{\boldsymbol{\mathscr{E}}} = \frac{1}{\mathscr{M}}(Q\dot{\boldsymbol{\mathscr{E}}} \times \boldsymbol{B}^{\text{ext}}), \tag{61}$$

and the magnetic field plays a strong role in the deviation of the trajectories. One can still expect rotation about the center-of-mass for the cluster due to term $\mathscr{T}_6$, which is dependent on $\bar{\boldsymbol{I}}_q$, in Equation (26), even when $\boldsymbol{R}_q=\boldsymbol{0}$.

6. CLOSING REMARKS

It was shown that Equations (25) and (26) govern the dynamics of a charged cluster, and that the following three quantities play a central role in the cluster behavior:

- the sum of the individual (q_i) charges: $Q \stackrel{\text{def}}{=} \sum_{i=1}^{N_c} q_i$ ('overall charge' or the first moment),
- the sum of the distances between the individual charged particles ($\boldsymbol{r}_i$) and the center-of-mass of the cluster ($\boldsymbol{r}_{\text{cm}}$), weighted by the individual charges: $\boldsymbol{R}_q \stackrel{\text{def}}{=} \sum_{i=1}^{N_p} q_i(\boldsymbol{r}_i - \boldsymbol{r}_{\text{cm}})$ ('charged radius' or the second-moment) and

DOI: 10.1002/nme

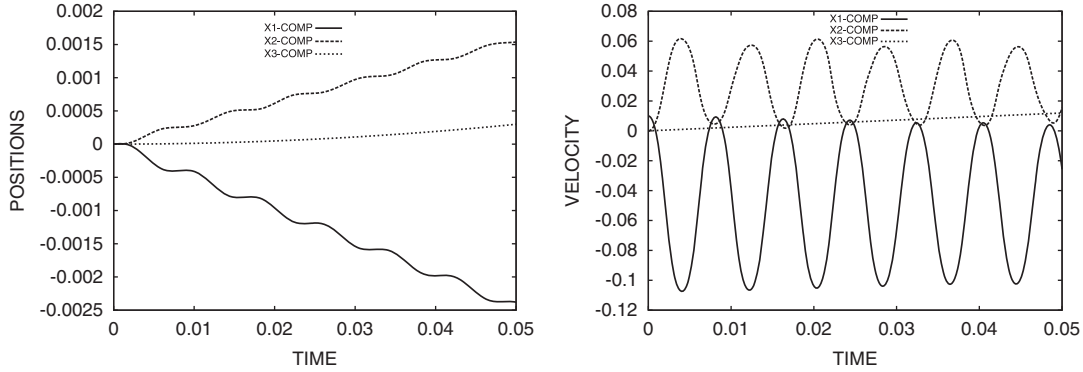

Figure 9. General case 3: $\boldsymbol{v}(t=0)=0.01\boldsymbol{e}_1$, $\boldsymbol{B}^{\text{ext}}=0.01\boldsymbol{e}_3$ and $\boldsymbol{E}^{\text{ext}}=0.1\boldsymbol{e}_3$. LEFT: the position of the center-of-mass. RIGHT: the velocity of the center-of-mass.

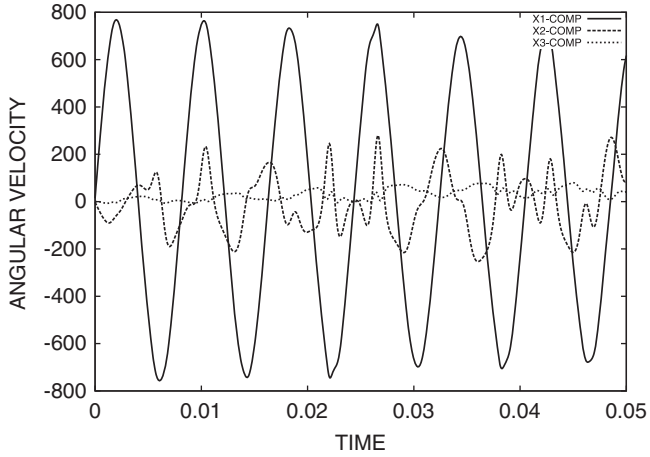

Figure 10. General case 3: $\boldsymbol{v}(t=0)=0.01\boldsymbol{e}_1$, $\boldsymbol{B}^{\text{ext}}=0.01\boldsymbol{e}_3$ and $\boldsymbol{E}^{\text{ext}}=0.1\boldsymbol{e}_3$: the angular velocity.

- the sum of the self-cross-product of the distances between the individual charged particles and the center-of-mass of the cluster, weighted by the individual charges ($\bar{\boldsymbol{I}}_q$): $\boldsymbol{H}_q=\bar{\boldsymbol{I}}_q\cdot\boldsymbol{\omega}\stackrel{\text{def}}{=}\sum_{i=1}^{N_p} q_i(\boldsymbol{r}_i-\boldsymbol{r}_{\text{cm}})\times\boldsymbol{\omega}\times(\boldsymbol{r}_i-\boldsymbol{r}_{\text{cm}})$, where $\boldsymbol{\omega}$ is the angular velocity of the body and $\bar{\boldsymbol{I}}_q$ has components of $(p,s=1,2,3)$ $\bar{I}_{q,ps}=\sum_{i=1}^{N_c} q_i(\|\boldsymbol{r}_i-\boldsymbol{r}_{\text{cm}}\|^2\delta_{ps}-\hat{x}_{ip}\hat{x}_{is})$ ('moment of charge' or the third-moment).

In addition to dictating the motion of a cluster, these quantities control the differences in the motion of a charged cluster relative to that of a single charged particle. The deviation in dynamics of a charged cluster and a single charged particle (or lumped charged mass) is strongly influenced by the simultaneous presence of an electric and magnetic field; in particular for large off-center charges, characterized by $\boldsymbol{R}_q$ and $\bar{\boldsymbol{I}}_q$, the motion will vary significantly, and is governed by Equation (55).

DOI: 10.1002/nme

Independent of the purely scientific interest in the dynamics of a charged cluster, there are implications of these results for large-scale computation of particulate flows. Within the last decade, simultaneous advances in computational methods, applied mathematics and high-performance computing have raised the possibility that an analyst can directly numerically simulate (DNS) a process employing particulate flows containing several million particles, incorporating all of the important microscale details. A relatively straightforward DNS-type formulation of the dynamics of a multi-particulate system is to track the motion of $i = 1, 2 \ldots N$ particles,

$$m_i \ddot{\boldsymbol{r}}_i = \boldsymbol{\psi}_i^{\text{tot}}(\boldsymbol{r}_1, \boldsymbol{r}_2, \ldots, \boldsymbol{r}_{N_p}) = \boldsymbol{\psi}_i^{\text{nf}} + \boldsymbol{\psi}_i^{\text{con}} + q_i(\boldsymbol{E}^{\text{ext}} + \boldsymbol{v}_i \times \boldsymbol{B}^{\text{ext}}), \tag{62}$$

where $\boldsymbol{r}_i$ is the position vector of the ith particle, $\boldsymbol{\psi}_i^{\text{tot}}$ represents all forces acting on particle i, $\boldsymbol{\psi}_i^{\text{nf}}$ represents near-field inter-(charged)particle forces acting on particle i, $\boldsymbol{\psi}_i^{\text{con}}$ represents contact forces acting on particle i and $\boldsymbol{E}^{\text{ext}}$ and $\boldsymbol{B}^{\text{ext}}$ are the external electromagnetic fields. The simulation of such flowing particulate systems has been extensively investigated for the last decade by Zohdi [15–24], employing numerical schemes based on high-performance iterative solvers, sorting-binning for fast inter-particle calculations, Verlet lists, domain decomposition, parallel processing and temporally adaptive methods. These types of formulations can easily describe the interaction of multiple particulate jets, jet breakup/disintegration and jet impact, where the application of continuum approaches is extremely difficult. The dynamics of clusters that evolve within a jet can be represented by directly describing the motion of each individual particle, with the appropriate binding conditions (constraints) to its neighbors in the cluster. This results in N_{c} (number of particles in the cluster) vector-valued equations for the cluster (one for each coordinate component). However, the representation as a cluster leads to two vector-valued equations (three scalar equations for translation and three for rotation), and is a significant reduction of computational effort. One must keep in mind that the cost of solving this rigid-body system is insignificant compared with a flowing particle problem with thousands of degrees of freedom, contact searches, etc. The blending of cluster-equations and those for loose particles, in order to model clusters co-existing with free-flowing particulates within a system, can significantly reduce computational size of the simulation. This is currently under investigation by the author.

APPENDIX A: TIME-STEPPING SCHEMES

A.1. Generic trapezoidal methods

Consider a generic second-order system describing the equation of motion of a particle i

$$m_i \dot{\boldsymbol{v}}_i = \boldsymbol{\psi}_i^{\text{tot}}, \tag{A1}$$

where $\boldsymbol{\psi}_i^{\text{tot}}$ is the total force provided from interactions with the external environment. Expanding the velocity in a Taylor series about $t + \phi\Delta t$, we obtain

$$\boldsymbol{v}_i(t + \Delta t) = \boldsymbol{v}_i(t + \phi\Delta t) + \frac{\mathrm{d}\boldsymbol{v}_i}{\mathrm{d}t}|_{t+\phi\Delta t}(1-\phi)\Delta t + \frac{1}{2}\frac{\mathrm{d}^2\boldsymbol{v}_i}{\mathrm{d}t^2}|_{t+\phi\Delta t}(1-\phi)^2(\Delta t)^2 + \mathcal{O}(\Delta t)^3 \tag{A2}$$

and

$$\boldsymbol{v}_i(t) = \boldsymbol{v}_i(t + \phi\Delta t) - \frac{\mathrm{d}\boldsymbol{v}_i}{\mathrm{d}t}|_{t+\phi\Delta t}\phi\Delta t + \frac{1}{2}\frac{\mathrm{d}^2\boldsymbol{v}_i}{\mathrm{d}t^2}|_{t+\phi\Delta t}\phi^2(\Delta t)^2 + \mathcal{O}(\Delta t)^3. \tag{A3}$$

DOI: 10.1002/nme

Subtracting the two expressions yields

$$\left.\frac{\mathrm{d}\boldsymbol{v}_i}{\mathrm{d}t}\right|_{t+\phi\Delta t} = \frac{\boldsymbol{v}_i(t+\Delta t)-\boldsymbol{v}_i(t)}{\Delta t}+\hat{\mathcal{O}}(\Delta t), \tag{A4}$$

where $\hat{\mathcal{O}}(\Delta t)=\mathcal{O}(\Delta t)^2$, when $\phi=\frac{1}{2}$. Thus, inserting this into the equations of equilibrium yields

$$\boldsymbol{v}_i(t+\Delta t)=\boldsymbol{v}_i(t)+\frac{\Delta t}{m_i}\boldsymbol{\psi}_i^{\mathrm{tot}}(t+\phi\Delta t)+\hat{\mathcal{O}}(\Delta t)^2. \tag{A5}$$

Note that adding a weighted sum of equations (A2) and (A3) yields

$$\boldsymbol{v}_i(t+\phi\Delta t)=\phi\boldsymbol{v}_i(t+\Delta t)+(1-\phi)\boldsymbol{v}_i(t)+\mathcal{O}(\Delta t)^2, \tag{A6}$$

which will be useful shortly. Now expanding the position of the center-of-mass in a Taylor series about $t+\phi\Delta t$, we obtain

$$\boldsymbol{r}_i(t+\Delta t)=\boldsymbol{r}_i(t+\phi\Delta t)+\left.\frac{\mathrm{d}\boldsymbol{r}_i}{\mathrm{d}t}\right|_{t+\phi\Delta t}(1-\phi)\Delta t+\frac{1}{2}\left.\frac{\mathrm{d}^2\boldsymbol{r}_i}{\mathrm{d}t^2}\right|_{t+\phi\Delta t}(1-\phi)^2(\Delta t)^2+\mathcal{O}(\Delta t)^3 \tag{A7}$$

and

$$\boldsymbol{r}_i(t)=\boldsymbol{r}_i(t+\phi\Delta t)-\left.\frac{\mathrm{d}\boldsymbol{r}_i}{\mathrm{d}t}\right|_{t+\phi\Delta t}\phi\Delta t+\frac{1}{2}\left.\frac{\mathrm{d}^2\boldsymbol{r}_i}{\mathrm{d}t^2}\right|_{t+\phi\Delta t}\phi^2(\Delta t)^2+\mathcal{O}(\Delta t)^3. \tag{A8}$$

Subtracting the two expressions yields

$$\frac{\boldsymbol{r}_i(t+\Delta t)-\boldsymbol{r}_i(t)}{\Delta t}=\boldsymbol{v}_i(t+\phi\Delta t)+\hat{\mathcal{O}}(\Delta t). \tag{A9}$$

Inserting Equation (A6) yields

$$\boldsymbol{r}_i(t+\Delta t)=\boldsymbol{r}_i(t)+(\phi\boldsymbol{v}_i(t+\Delta t)+(1-\phi)\boldsymbol{v}_i(t))\Delta t+\hat{\mathcal{O}}(\Delta t)^2, \tag{A10}$$

and thus using Equation (A5) we have

$$\boldsymbol{r}_i(t+\Delta t)=\boldsymbol{r}_i(t)+\boldsymbol{v}_i(t)\Delta t+\frac{\phi(\Delta t)^2}{m_i}\boldsymbol{\psi}_i^{\mathrm{tot}}(t+\phi\Delta t)+\hat{\mathcal{O}}(\Delta t)^2. \tag{A11}$$

The term $\boldsymbol{\psi}_i^{\mathrm{tot}}(t+\phi\Delta t)$ can be handled in two main ways:

- $\boldsymbol{\psi}_i^{\mathrm{tot}}(t+\phi\Delta t)\approx\boldsymbol{\psi}_i^{\mathrm{tot}}(\phi\boldsymbol{r}_i(t+\Delta t)+(1-\phi)\boldsymbol{r}_i(t))$ or
- $\boldsymbol{\psi}_i^{\mathrm{tot}}(t+\phi\Delta t)\approx\phi\boldsymbol{\psi}_i^{\mathrm{tot}}(\boldsymbol{r}_i(t+\Delta t))+(1-\phi)\boldsymbol{\psi}_i^{\mathrm{tot}}(\boldsymbol{r}_i(t))$.

The differences are quite minute between either of the above; thus, for brevity, we choose the latter. In summary, we have the following:

$$\boldsymbol{r}_i(t+\Delta t)=\boldsymbol{r}_i(t)+\boldsymbol{v}_i(t)\Delta t+\frac{\phi(\Delta t)^2}{m_i}(\phi\boldsymbol{\psi}_i^{\mathrm{tot}}(\boldsymbol{r}_i(t+\Delta t))+(1-\phi)\boldsymbol{\psi}^{\mathrm{tot}}(\boldsymbol{r}_i(t)))+\hat{\mathcal{O}}(\Delta t)^2, \tag{A12}$$

DOI: 10.1002/nme

where

- when $\phi=1$, then this is the (implicit) Backward Euler scheme, which is very stable (very dissipative) and $\hat{\mathcal{O}}(\Delta t)^2=\mathcal{O}(\Delta t)^2$ locally in time,
- when $\phi=0$, then this is the (explicit) Forward Euler scheme, which is conditionally stable and $\hat{\mathcal{O}}(\Delta t)^2=\mathcal{O}(\Delta t)^2$ locally in time and
- when $\phi=0.5$, then this is the (implicit) 'Midpoint' scheme, which is stable and $\hat{\mathcal{O}}(\Delta t)^2=\mathcal{O}(\Delta t)^3$ locally in time.

A.2. Adaptive time-stepping methods

Equation (A12) can be solved recursively by recasting the relation as

$$\boldsymbol{r}_i^{L+1,K}=\mathcal{G}(\boldsymbol{r}_i^{L+1,K-1})+\mathcal{R}_i, \tag{A13}$$

where $K=1,2,3,\ldots$ is the index of iteration within time-step $L+1$ and $\mathcal{R}_i$ is a remainder term that does not depend on the solution, i.e.

$$\mathcal{R}_i\neq\mathcal{R}_i(\boldsymbol{r}_1^{L+1},\boldsymbol{r}_2^{L+1}\ldots\boldsymbol{r}_N^{L+1}). \tag{A14}$$

The convergence of such a scheme is dependent on the behavior of $\mathcal{G}$. Namely, a sufficient condition for convergence is that $\mathcal{G}$ is a contraction mapping for all $\boldsymbol{r}_i^{L+1,K}$, $K=1,2,3\ldots$ In order to investigate this further, we define the iteration error as

$$\varpi_i^{L+1,K}\stackrel{\text{def}}{=}\boldsymbol{r}_i^{L+1,K}-\boldsymbol{r}_i^{L+1}. \tag{A15}$$

A necessary restriction for convergence is iterative self consistency, i.e. the 'exact' (discretized) solution must be represented by the scheme

$$\mathcal{G}(\boldsymbol{r}_i^{L+1})+\mathcal{R}_i=\boldsymbol{r}_i^{L+1}. \tag{A16}$$

Enforcing this restriction, a sufficient condition for convergence is the existence of a contraction mapping

$$\|\underbrace{\boldsymbol{r}_i^{L+1,K}-\boldsymbol{r}_i^{L+1}}_{\varpi_i^{L+1,K}}\|=\|\mathcal{G}(\boldsymbol{r}_i^{L+1,K-1})-\mathcal{G}(\boldsymbol{r}_i^{L+1})\|\leqslant\eta^{L+1,K}\|\boldsymbol{r}_i^{L+1,K-1}-\boldsymbol{r}_i^{L+1}\|,$$

where, if $0\leqslant\eta^{L+1,K}<1$ for each iteration K, then $\varpi_i^{L+1,K}\rightarrow\boldsymbol{0}$ for any arbitrary starting value $\boldsymbol{r}_i^{L+1,K=0}$, as $K\rightarrow\infty$. This type of contraction condition is sufficient, but not necessary, for convergence. Explicitly, the recursion is

$$\boldsymbol{r}_i^{L+1,K}=\underbrace{\boldsymbol{r}_i^L+\boldsymbol{v}_i^L\Delta t+\frac{\phi(1-\phi)(\Delta t)^2}{m_i}\boldsymbol{\psi}_i^{\text{tot},L}}_{\mathcal{R}}+\underbrace{\frac{\phi^2(\Delta t)^2}{m_i}\boldsymbol{\psi}_i^{\text{tot},L+1,K-1}}_{\mathcal{G}(\boldsymbol{r}_i^{L+1,K-1})}, \tag{A17}$$

where

$$\boldsymbol{\psi}_i^{\text{tot},L}\stackrel{\text{def}}{=}\boldsymbol{\psi}_i^{\text{tot},L}(\boldsymbol{r}_1^L,\boldsymbol{r}_2^L\ldots\boldsymbol{r}_N^L) \tag{A18}$$

DOI: 10.1002/nme

and

$$\boldsymbol{\psi}_i^{\text{tot},L+1,K-1} \stackrel{\text{def}}{=} \boldsymbol{\psi}_i^{\text{tot},L+1,K-1}(\boldsymbol{r}_1^{L+1,K-1}, \boldsymbol{r}_2^{L+1,K-1} \ldots \boldsymbol{r}_N^{L+1,K-1}). \tag{A19}$$

The convergence of Equation (A17) is scaled by

$$\eta \propto \frac{(\phi \Delta t)^2}{m_i}. \tag{A20}$$

Therefore, we see that the contraction constant of $\mathscr{G}$ is (1) directly dependent on the strength of the interaction forces, (2) inversely proportional to m and (3) directly proportional to $(\Delta t)^2$ (at time $= t$). Therefore, if convergence is slow within a time-step, the time-step size, which is adjustable, can be reduced by an appropriate amount to increase the rate of convergence. Thus, decreasing the time-step size improves the convergence; however, we want to simultaneously maximize the time-step sizes to decrease overall computing time, while still meeting an error tolerance on the numerical solution's accuracy. In order to achieve this goal, we follow approaches found in Zohdi [16–19, 22–24] originally developed for continuum thermo-chemical multifield problems [37], in which (1) one approximates

$$\eta^{L+1,K} \approx S(\Delta t)^p \tag{A21}$$

(S is a constant) and (2) one assumes the error within an iteration to behave according to

$$(S(\Delta t)^p)^K \varpi^{L+1,0} = \varpi^{L+1,K}, \tag{A22}$$

$K = 1, 2, \ldots,$ where $\varpi^{L+1,0}$ is the initial norm of the iterative error and S is intrinsic to the system.*** Our goal is to meet an error tolerance in exactly a preset number of iterations. To this end, one writes

$$(S(\Delta t_{\text{tol}})^p)^{K_{\text{d}}} \varpi^{L+1,0} = \text{TOL}, \tag{A23}$$

where TOL is a tolerance and where K_{d} is the number of desired iterations.Typically, K_{d} is chosen to be between 5 and 10 iterations. If the error tolerance is not met in the desired number of iterations, the contraction constant $\eta^{L+1,K}$ is too large. Accordingly, one can solve for a new smaller step size, under the assumption that S is constant,

$$\Delta t_{\text{tol}} = \Delta t \left(\frac{\left(\dfrac{\text{TOL}}{\varpi^{L+1,0}} \right)^{1/(pK_{\text{d}})}}{\left(\dfrac{\varpi^{L+1,K}}{\varpi^{L+1,0}} \right)^{1/(pK)}} \right). \tag{A24}$$

The assumption that S is a constant is not critical, since the time-steps are to be recursively refined and unrefined throughout the simulation. Clearly, the expression in Equation (A24) can also be used for time-step enlargement, if convergence is met in less than K_{d} iterations.

***For the class of problems under consideration, due to the quadratic dependency on Δt, $p \approx 2$.

DOI: 10.1002/nme

A.3. Adaptive time-stepping methods

For the specific cluster problem at hand, the algorithm is as follows:

(1) GLOBAL FIXED-POINT ITERATION: (SET $K=0$):

(2) COMPUTE $\boldsymbol{r}_{\mathrm{cm}}^{L+1,K}$ AND $\boldsymbol{\omega}_{\mathrm{cm}}^{L+1,K}$

(3) POST-PROCESS $\boldsymbol{r}_i^{L+1,K}$, $i=1,2\ldots N_{\mathrm{c}}$

(4) ERROR MEASURE/TIME-STEP ADAPTIVITY: (SEE APPENDIX)

$$(a)\varpi_K \stackrel{\mathrm{def}}{=} \frac{\sum_{i=1}^{N_{\mathrm{c}}} \|\boldsymbol{r}_i^{L+1,K}-\boldsymbol{r}_i^{L+1,K-1}\|}{\sum_{i=1}^{N_{\mathrm{c}}} \|\boldsymbol{r}_i^{L+1,K}-\boldsymbol{r}_i^{L}\|} \qquad \text{(normalized)}$$

$$(b)Z_K \stackrel{\mathrm{def}}{=} \frac{\varpi_K}{TOL_r}$$

$$(c)\Phi_K \stackrel{\mathrm{def}}{=} \left(\frac{\left(\frac{TOL}{\varpi_0}\right)^{\frac{1}{pK_{\mathrm{d}}}}}{\left(\frac{\varpi_K}{\varpi_0}\right)^{\frac{1}{pK}}} \right) \qquad \text{(time-scaling)} \tag{A25}$$

(5) IF TOLERANCE MET ($Z_K \leqslant 1$) AND $K<K_{\mathrm{d}}$ THEN:

(a) INCREMENT TIME: $t=t+\Delta t$

(b) CONSTRUCT NEW TIME STEP: $(\Delta t)^{new}=\Phi_K(\Delta t)^{old}$,

(c) SELECT MINIMUM: $\Delta t = MIN((\Delta t)^{lim},(\Delta t)^{new})$ AND GO TO (1)

(6) IF TOLERANCE NOT MET ($Z_K>1$) AND $K=K_{\mathrm{d}}$ THEN:

(a) CONSTRUCT NEW TIME STEP: $(\Delta t)^{new}=\Phi_K(\Delta t)^{old}$

(b) RESTART AT TIME = t AND GO TO (1)

Remark

Variants of the adaptive time-scaling used above have been developed in Zohdi [16–20, 22–24].

REFERENCES

1. Luo L, Dornfeld DA. Material removal mechanism in chemical mechanical polishing: theory and modeling. *IEEE Transaction*: *Semiconductor Manufacturing* 2001; **14**(2):112–133.
2. Luo L, Dornfeld DA. Effects of abrasive size distribution in chemical–mechanical planarization: modeling and verification. *IEEE Transaction*: *Semiconductor Manufacturing* 2003; **16**:469–476.
3. Luo L, Dornfeld DA. Material removal regions in chemical mechanical planarization for sub-micron integration for sub-micron integrated circuit fabrication: coupling effects of slurry chemicals, abrasive size distribution, and wafer–pad contact area. *IEEE Transaction*: *Semiconductor Manufacturing* 2003; **16**:45–56.

DOI: 10.1002/nme

4. Luo L, Dornfeld DA. *Integrated Modeling of Chemical Mechanical Planarization of Sub-micron IC Fabrication*. Springer: Berlin, 2004.
5. Arbelaez D, Zohdi TI, Dornfeld D. Modeling and simulation of material removal with particulate flow. *Computational Mechanics* 2008; **42**:749–759.
6. Arbelaez D, Zohdi TI, Dornfeld D. On impinging near-field granular jets. *International Journal for Numerical Methods in Engineering* 2009; **80**(6):815–845.
7. Ciampini D, Spelt JK, Papini M. Simulation of interference effects in particle streams following impact with a flat surface. Part I. Theory and analysis. *Wear* 2003; **254**:237–249.
8. Ciampini D, Spelt JK, Papini M. Simulation of interference effects in particle streams following impact with a flat surface. Part II. Parametric study and implications for erosion testing and blast cleaning. *Wear* 2003; **254**:250–264.
9. Gomes-Ferreira C, Ciampini D, Papini M. The effect of inter-particle collisions in erosive streams on the distribution of energy flux incident to a flat surface. *Tribology International* 2004; **37**:791–807.
10. Ghobeity A, Spelt JK, Papini M. Abrasive jet micro-machining of planar areas and transitional slopes. *Journal of Micromechanics and Microengineering* 2008; **18**:055014.
11. Ghobeity A, Krajac T, Burzynski T, Papini M, Spelt JK. Surface evolution models in abrasive jet micromachining. *Wear* 2008; **264**:185–198.
12. Torquato S. *Random Heterogeneous Materials*: *Microstructure and Macroscopic Properties*. Springer: New York, 2002.
13. Ghosh S, Valiveti DM, Harris SH, Boileau J. Microstructure characterization based domain partitioning as a pre-processor to multi-scale modeling of cast Aluminum alloys. *Modeling and Simulation in Materials Science and Engineering* 2006; **14**:1363–1396.
14. Fish J. Bridging the scales in nano engineering and science. *Journal of Nanoparticle Research* 2006; **8**:577–594.
15. Zohdi TI. Large-scale statistical inverse computation of inelastic accretion in transient granular flows. *International Journal of Nonlinear Mechanics* 2003; **8**(38):1205–1219.
16. Zohdi TI. Computational design of swarms. *International Journal for Numerical Methods in Engineering* 2003; **57**:2205–2219.
17. Zohdi TI. Modeling and direct simulation of near-field granular flows. *International Journal of Solids and Structures* 2004; **42**(2): 539–564.
18. Zohdi TI. A computational framework for agglomeration in thermo-chemically reacting granular flows. *Proceedings of the Royal Society* 2004; **460**(2052):3421–3445.
19. Zohdi TI. Charge-induced clustering in multifield particulate flow. *International Journal for Numerical Methods in Engineering* 2005; **62**(7):870–898.
20. Zohdi TI. Computation of strongly coupled multifield interaction in particle–fluid systems. *Computer Methods in Applied Mechanics and Engineering* 2007; **196**:3927–3950.
21. Zohdi TI. Particle collision and adhesion under the influence of near-fields. *Journal of Mechanics of Materials and Structures* 2007; **2**(6):1011–1018.
22. Zohdi TI. *Introduction to the Modeling and Simulation of Particulate Flows*. SIAM (Society for Industrial and Applied Mathematics): Philadelphia, PA, 2007.
23. Zohdi TI. Mechanistic modeling of swarms. *Computer Methods in Applied Mechanics and Engineering* 2009; **198**(21–26):2039–2051.
24. Zohdi TI. On the dynamics of charged electromagnetic particulate jets. *Archives of Computational Methods in Engineering* 2010; **17**(2):109–135.
25. Frenklach M, Carmer CS. Molecular dynamics using combined quantum & empirical forces: application to surface reactions. *Advances in Classical Trajectory Methods* 1999; **4**:27–63.
26. Haile JM. *Molecular Dynamics Simulations*: *Elementary Methods*. Wiley: New York, 1992.
27. Hase WL. *Molecular Dynamics of Clusters*, *Surfaces*, *Liquids*, *and Interfaces*. Advances in Classical Trajectory Methods, vol. 4. JAI Press, 1999.
28. Schlick T. *Molecular Modeling and Simulation. An Interdisciplinary Guide*. Springer: New York, 2000.
29. Rapaport DC. *The Art of Molecular Dynamics Simulation*. Cambridge University Press: Cambridge, 1995.
30. Torquato S. Inverse optimization techniques for targeted self-assembly. *Soft Matter* 2009; **5**:1157.
31. Rechtsman M, Stillinger FH, Torquato S. Designed interaction potentials via inverse methods for self-assembly. *Physical Review E* 2006; **73**:011406.
32. Rechtsman M, Stillinger FH, Torquato S. Optimized interactions for targeted self-assembly: application to honeycomb lattice. *Physical Review Letters* 2005; **95**:228301.

DOI: 10.1002/nme

33. Moelwyn-Hughes EA. *Physical Chemistry*. Pergamon: Oxford, 1961.
34. Stillinger FH, Weber TA. Computer simulation of local order in condensed phases of silicon. *Physical Review B* 1985; **31**:5262–5271.
35. Tersoff J. Empirical interatomic potential for carbon, with applications to amorphous carbon. *Physical Review Letters* 1988; **61**:2879–2882.
36. Jackson JD. *Classical Electrodynamics* (3rd edn). Wiley: New York, 1998.
37. Zohdi TI. An adaptive-recursive staggering strategy for simulating multifield coupled processes in micro-heterogeneous solids. *International Journal for Numerical Methods in Engineering* 2002; **53**:1511–1532.

DOI: 10.1002/nme